

F₂ laser ablation of UV transparent polymer material

Kotaro OBATA, Koji SUGIOKA, and Katsumi MIDORIKAWA

RIKEN (The institute of physical and chemical research)
Hirosawa 2-1, Wako, Saitama 351-0198, Japan
E-mail: E-mail: kobata@riken.jp

Precise microfabrication of amorphous fluorine-polymer (CYTOP), which is highly transparent in the wavelength range from 200 nm to 2 μm has been demonstrated by F₂ laser ($\lambda > 157$ nm). F₂ laser ablation achieves well-defined micro-patterning with little thermal effect and little debris deposition at etched area. The etching rate linearly increases with number of pulses and logarithm of laser fluence. The F₂ laser ablation of CYTOP proceeds by single-photon absorption and its effective absorption coefficient is approximately $\sim 10^5 \text{ cm}^{-1}$. On the other hand, KrF ($\lambda = 248$ nm), ArF ($\lambda = 193$ nm) excimer laser, and femtosecond laser ($\lambda = 775$ nm, $\tau = 180$ fs) can not perform high-quality ablation due to excellent transparency of CYTOP. Etched area ablated by F₂ laser shows no visible change, while the other lasers induce color change to black. It is deduced that the color change is responsible for carbonization due to thermal effect induced by multiphoton absorption.

Keywords: F₂ laser, VUV, polymer, CYTOP, ablation, micromachine

1. Introduction

A transparent polymer from UV to near IR is getting an alternative of glass materials as substrate for device of opto-electronics, bio-photonics, data storage, and micro total analysis system (μ -TAS) since it is light and highly flexible. Some of commercially available polymers such as polymethylmethacrylate (acrylic or PMMA), polycarbonate (PC), and polyethylene terephthalate (PET) have excellent transparency from near-UV to UV above 300 nm in wavelength. However, few polymers can transmit in deep-UV region shorter than 300 nm. Search of the deep-UV transparent polymer and development of microfabrication technique of such a material are of great use for micro-optical device and μ -TAS working at UV range. One of candidates is an amorphous fluorine-polymer named CYTOP developed by Asahi glass Co. Ltd. [1,2]. The transmittance of CYTOP is more than 90% from 200 nm to 2 μm . Additionally, the CYTOP has high-chemical resistance to acids, alkalis, and organic solvents. Furthermore it can be used as high-electrical insulation film due to its high permittivity [1]. So far, some groups have fabricated optical waveguide [3,4], fiber and fiber grating [5-10], optical device for neutrons [11], micro-device [12,13], and μ -TAS [14-16] by

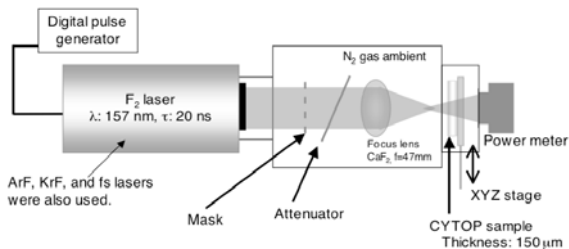


Fig. 1 Schematic illustration of experimental setup for CYTOP ablation using F₂ laser.

using CYTOP. Although plasma or ion etching is utilized for etching of CYTOP, a conventional photo-resist process can not be used for micro-patterning due to low adhesion between CYTOP and resist material. Therefore, development of high-quality and high-efficiency microfabrication technique is highly desired. In this paper, we demonstrate precise microfabrication of CYTOP film by using F₂ laser ablation with high-photon energy of 7.9 eV, since F₂ laser has strong absorption to CYTOP.

2. Experimental procedure

A schematic illustration of experimental setup for CYTOP ablation by F₂ laser is shown in Fig. 1. The optical grade CYTOP film was used as the sample. The CYTOP sample was placed on PC controlled XYZ stage set in the ablation chamber to scan a F₂ laser beam. The ablation chamber was filled with dry nitrogen gas ambient to prevent an absorption of F₂ laser beam from oxygen. F₂ laser beam through a metal stencil mask was projected on the

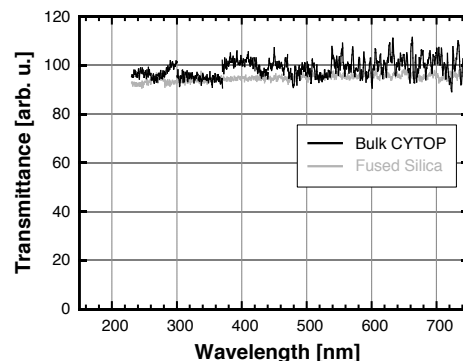


Fig. 2 Transmittance spectra of CYTOP film used in this study and UV grade fused silica.

sample surface at 1 Hz. For comparison, KrF excimer laser ($\lambda=248$ nm, $\tau=34$ ns, repetition rate= 1 Hz), ArF excimer laser ($\lambda=193$ nm, $\tau=20$ ns, Repetition rate= 1 Hz), femto-second (fs) laser ($\lambda=775$ nm, $\tau=180$ fs, repetition rate= 1 kHz) were also used. Transmittance spectrum of CYTOP film used in this study is shown in Fig. 2. The spectrum of fused silica is also shown in Fig. 2 for reference. The transmittance of CYTOP has little difference from that of fused silica from 230 to 750 nm. Additionally, it was confirmed that CYTOP is also transparent to ArF excimer laser whose wavelength is 193 nm. Therefore, the CYTOP has

possibility to replace fused silica as the substrate of optical device working in UV region. The ablated patterns were observed by atomic force microscope (AFM) and optical microscope. The etched depth was measured by a surface profiler (α -step, KLA Tencor Co. Ltd.).

3. Results and discussion

Figure 3 shows optical microscope images of the CYTOP ablated by (a) KrF excimer laser at laser fluence of 3.0 J/cm^2 and 10 pulses, (b) ArF excimer laser at laser fluence of 4.0 J/cm^2 and 10 pulses, and (c) fs laser at peak intensity of $8.3 \times 10^{17} \text{ W/cm}^2$ and laser scanning speed of 1 mm/sec, respectively. For KrF excimer laser ablation, the ablated pattern is quite irregular, which does not correspond to the irradiated pattern of laser beam in the least. In addition, the ablation area is greatly roughened and changed to black color and debris is observed around the ablated area. This coloring might be occurred by carbonization due to thermal effect induced by multiphoton absorption of KrF excimer laser beam. For ArF excimer laser ablation, the ablated pattern is a little bit improved as compared with KrF excimer laser ablation, however, still irregular. The transparency also disappears, and black color debris is observed around the ablated area. Since CYTOP has little absorption to a wavelength of 193 nm, ablation using ArF excimer laser should take place by multiphoton absorption. Therefore, the thermal effect cannot be ignored even for ArF excimer laser, resulting in carbonization. In the mean while, it is well known that ultrashort pulse laser can improve ablation quality of any transparent material compared with nanosecond lasers by reducing the thermal effect. In fact, the pattern ablated by fs laser seems to be much better than excimer lasers, but the ablated sur-

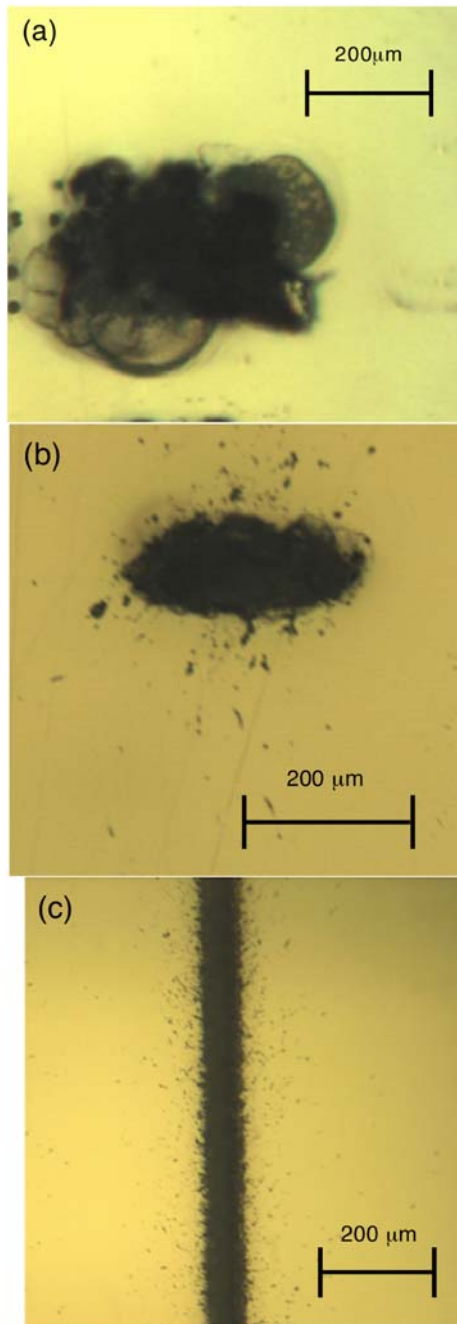


Fig. 3 Optical microscope images of CYTOP surface ablated by (a) KrF excimer laser (laser fluence: 3.0 J/cm^2) (b) ArF excimer laser (laser fluence: 4.0 J/cm^2), and (c) femtosecond laser (Intensity: $8.3 \times 10^{17} \text{ W/cm}^2$, scan speed: 1 mm/sec).

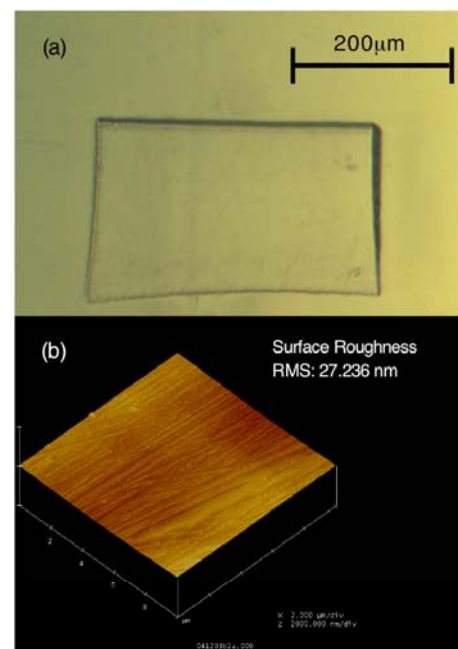


Fig. 4 (a) Optical microscope image and (b) AFM image of CYTOP ablated by F_2 laser at laser fluence of 157 mJ/cm^2 .

face became black color even for the fs laser ablation. This might be due to heat accumulation by high repetition rate of 1 kHz.

On the other hand, Fig. 4 shows (a) the optical microscope image and (b) AFM image of CYTOP ablated by F₂ laser. 10 shots of F₂ laser pulse were irradiated to the CYTOP sample at 157 mJ/cm² of laser fluence and 1 Hz repetition rate. The etching quality is drastically improved compared with other lasers used in Fig 3. No color change is observed at the ablated area and high-transparency is maintained. From AFM measurement, root mean square (RMS) of surface roughness is estimated to be approximately 27 nm. The roughness at etched area becomes 6 times larger than that of untreated CYTOP sample. However, this roughness is enough small for optical micro-device and μ-TAS applications.

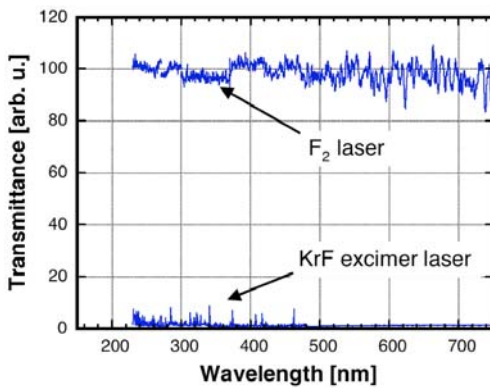


Fig. 5 Transmission spectra at the area ablated by KrF excimer laser and F₂ laser.

One of key issues for device manufacture of UV transparent material is keeping its high-transparency at the processed regions. Figure 5 shows the transmittance spectra at the areas ablated by F₂ laser and KrF excimer laser, respectively. The transmittance spectrum of KrF excimer laser sample shows that etched area entirely loses the characteristic of high-transparency in the range of wavelength between 230 and 750 nm. This is attributed to carbonization by thermal effect induced by multiphoton absorption. While, little degradation of transparency is observed at the area etched by F₂ laser. The transmission loss of about 10 % in the analyzed range is due to reflection at the front and rear surfaces of the CYTOP sample, which is common for the untreated CYTOP. Therefore, F₂ laser ablation is promising as the optical device fabrication technique for CYTOP.

Figure 6 shows a variation of ablation rate of CYTOP film as a function of F₂ laser fluence. The ablation rate shows linear increase with the logarithm of the F₂ laser fluence. It is well known that the relationship between ablation rate *d* and laser fluence *F* in the case of single-photon absorption is expressed by

$$d = \frac{1}{\alpha_{eff}} \ln\left(\frac{F}{F_{th}}\right), (1)$$

where α_{eff} and F_{th} are the effective absorption coefficient and the ablation threshold laser fluence. Therefore, the linear increase of the ablation rate indicates that abla-

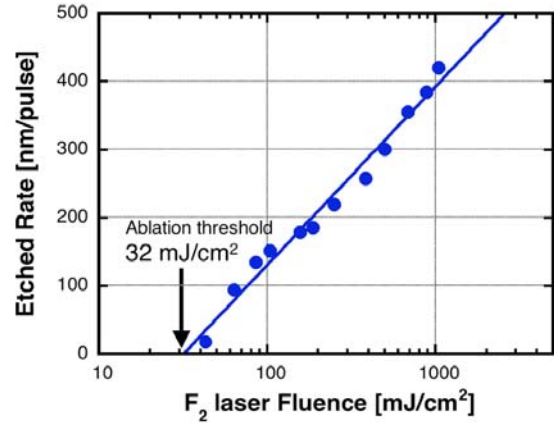


Fig. 6 Dependence of etching rate on F₂ laser fluence.

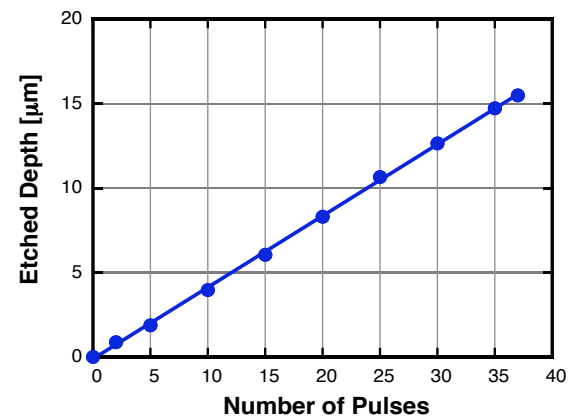


Fig. 7 Variation of the ablation depth of the CYTOP as a function of the number of F₂ laser pulse.

tion using F₂ laser is caused by the single-photon absorption. By extrapolation, the ablation threshold is estimated to be 32 mJ/cm². The effective absorption coefficient is estimated to be 8.80x10⁴ cm⁻¹. This large effective absorption coefficient is caused by high-photon energy of F₂ laser beam (7.9 eV), which is responsible for high-quality ablation.

Figure 7 shows variation of ablation depth of CYTOP as a function of the number of F₂ laser pulses. The F₂ laser was irradiated to the CYTOP at 1.0 J/cm² of laser fluence. The ablation depth linearly increases with increasing the number of F₂ laser pulses. This fact means that ablation proceeds with no incubation effect. The etching rate is estimated to be as high as 420 nm/pulse.

Figure 8 shows optical microscope images of CYTOP ablated by different number of pulses at 1.0 J/cm². Each sample shows clear etched area without color change to black and the ablation patterns are maintained for each pulse number. For samples irradiated at more than 15 shots, dark color region are observed. These are shadows produced by illumination of the optical microscope for the observation due to deep holes. Therefore, the transparency is maintained even after many pulse irradiation.

In the case of polymer ablation, laser beam is absorbed by chromophoric groups. Absorption of UV laser beam leads to electronic and vibrational excitation in the polymer materials resulting in photo-dissociation and abla-

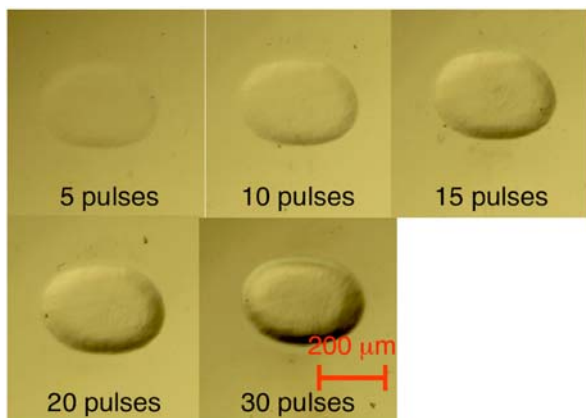


Fig. 8 Optical microscop images of the CYTOP etched at different numbers of F_2 laser pulses.

tion. For example of PTFE ablation, F_2 laser can lead to direct photo-dissociation of bond in the main chain of PTFE by single photon since photon energy of F_2 laser (182 kcal/mol) is larger than binding energy of that in PTFE (more than 160 kcal/mol). CYTOP has some dis-soluble bonds by F_2 laser, whose binding energy is in the range from 148 kcal/mol (ArF excimer laser) to 182 kcal/mol (F_2 laser). Optical absorption edge and absorbance were measured to be 170 nm and $1.9 \mu\text{m}^{-1}$ by French et. al. [17]. Therefore, direct photo-dissociation is possible by F_2 laser, leading to high-quality ablation of CYTOP

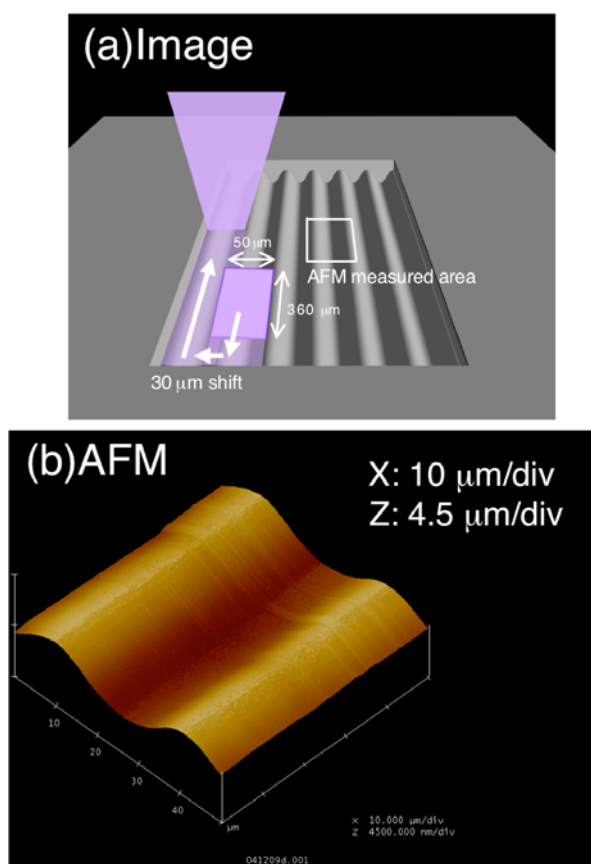


Fig. 9 (a) Schematic illustration of the laser scanning scheme and (b) AFM image of the fabricated micro-grating structure.

with little thermal effect.

A micro-grating structure was fabricated on the CYTOP surface by specific scanning of F_2 laser beam. Figure 9 shows (a) schematic illustration of the laser scanning scheme and (b) AFM image of the formed micro-grating structure. In order to forming the grating structure, rectangular shape F_2 laser beam (beam size: $50 \times 360 \mu\text{m}^2$) was scanned with lateral shift of $30 \mu\text{m}$. Namely, in this scheme, 40% of laser beam ($20 \mu\text{m}$) are overlapped with the area irradiated by previous scanning. Laser fluence was 260 mJ/cm^2 with scanning speed of $43 \mu\text{m/sec}$ (12% of $360 \mu\text{m}$) at 1Hz. The AFM image indicates that the sine curve-like micro-grating with approximately 30 micrometer period is formed. The etched depth is $2 \mu\text{m}$. Additionally, the micro-grating maintains smooth surface. In this experiment, the angle between bottom surface and the sidewall in etched area is not vertical. Therefore, the overlapped F_2 laser beam makes the sidewall smooth resulting in forming the sine curve-like micro-grating with smooth surface. The period of micro-grating can be shortened by reducing the beam shape.

4. Conclusion

High-quality microfabrication of the UV transparent polymer was demonstrated by F_2 laser. F_2 laser ablation can achieve high-quality ablation of CYTOP film without deterioration of transparency at etched area. The surface roughness at the etched area was as small as 27 nm. On the other hand, femtosecond laser, KrF, and ArF excimer lasers couldn't perform high-quality ablation and darkened the etched area. The etching rate of the F_2 laser ablation sample showed linear increase with the logarithm of the F_2 laser fluence. This dependence suggested that the ablation took place by single-photon absorption of F_2 laser beam. The ablation depth linearly increased with increasing number of F_2 laser pulses without any incubation effect and high-ablation rate over 400 nm/pulse was obtained. Fabrication of micro-grating with period of $30 \mu\text{m}$ on the CYTOP surface was successfully demonstrated. Thus, we conclude that F_2 laser ablation can be expected as efficient and high-quality microfabrication technique for CYTOP.

Acknowledgements

The authors would like to thank Dr. T. Shinohara for preparation of CYTOP sample and fruitful discussion.

References

- [1] <http://www.agc.co.jp/english/chemicals/shinsei/cytop/cytop.htm>
- [2] C. Anolick, J. A. Hrivnak, and R. C. Wheland, *Adv. Mat.* 10, 1211 (1998).
- [3] Y. G. Zhao, W. K. Lu, Y. Ma, S. S. Kim, S. T. Ho, and T. J. Marks, *Appl. Phys. Lett.*, 77, 2961 (2000).
- [4] A. M. Wu and A. Knoesen, *J. Polym. Sci. & Polym. Phys.* 39, 2717 (2001).
- [5] H. Y. Liu, G. D. Peng., P. L. Chu, Y. Koike, and Y. Watanabe, *Electron. Lett.*, 37, 347 (2001).

- [6] H. Y. Liu, G. D. Peng, and P. L. Chu, *Opt. Commun.* 204, 151 (2002).
- [7] F. Mederer, R. Jager, P. Schnitzer, H. Unold, M. Kicherer, K. J. Ebeling, M. Naritomi, and R. Yoshida, *Proc. SPIE* 3896, 273 (1999).
- [8] M. B. Tayahi, M. El-Aasser, and N. K. Dutta, *Proc. SPIE* 3939, 79 (2000).
- [9] G. D. Peng and P. L. Chu, *Proc. SPIE* 4110, 123 (2000).
- [10] J. Ballato, D. W. Smith Jr., S. H. Foulger, and E. Wagener, *Proc. SPIE* 4805, 1 (2002).
- [11] T. Shinohara, T. Adachi, K. Ikeda, T. Morishima, K. Hirota, H. M. Shimizu, T. Oku, and J. Suzuki, *Nucl. Instr. and Meth. A* 529, 134 (2004).
- [12] Y. Matsumoto, K. Yoshida, and M. Ishida, *Sensors & Actuators A*, 66, 308 (1998).
- [13] K. Maenaka, T. Nishimura, H. Ikeda, T. Fujita, and M. Maeda, *IEEJ Trans. on Sensors and Micromachines*, 120, 136 (2000).
- [14] S. Bhansali, A. Han, M. Patel, K. W. Oh, C. H. Ahn, and H. T. Henderson, *Proc. SPIE* 3877, 101 (1999).
- [15] N. Honda, S. Shoji, M. Isomura, Y. Ashihara, K. Akahori, and H. Sato, *Digest of Papers. Microprocesses and Nanotechnology 2001(MNC2001)*, pp.24
- [16] C. S. Lee, S. H. Lee, S. S. Park, Y. K. Kim, and B. G. Kim, *Biosensors Bioelectron.*, 18, 437 (2003).
- [17] R. H. French, R. C. Wheland, W. Qiu, M. F. Lemon, E. Zhang, J. Gordon, V. A. Petrov, V. F. Cherstkov, and N. I. Delaygina, *J. Fluorine Chem.*, 122, 63 (2003).

(Received: June 9, 2005, Accepted: September 22, 2005)